



Australian Government
**Australian Radiation Protection
and Nuclear Safety Agency**



Establishing radiation qualities in radiation (RQR), radiation qualities based on aluminium added filter (RQA) and radiation qualities based on copper added filter (RQT) beams

**Establishing radiation qualities in radiation
(RQR), radiation qualities based on
aluminium added filter (RQA) and radiation
qualities based on copper added filter
(RQT) beams**

March 2023

Dr Kam L Lee and Dr Duncan Butler

© Commonwealth of Australia 2023

This publication is protected by copyright. Copyright (and any other intellectual property rights, if any) in this publication is owned by the Commonwealth of Australia as represented by the Australian Radiation Protection and Nuclear Safety Agency (ARPANSA).



Creative Commons

With the exception of the Commonwealth Coat of Arms, any ARPANSA logos and any content that is marked as being third party material, this publication, *Establishing radiation qualities in radiation (RQR), radiation qualities based on aluminium added filter (RQA) and radiation qualities based on copper added filter (RQT) beams*, by the Australian Radiation Protection and Nuclear Safety Agency is licensed under a Creative Commons Attribution 3.0 Australia licence (to view a copy of the licence, visit <http://creativecommons.org/licenses/by/3.0/au>). It is a further condition of the licence that any numerical data referred to in this publication may not be changed. To the extent that copyright subsists in a third party, permission will be required from the third party to reuse the material.

In essence, you are free to copy, communicate and adapt the material as long as you attribute the work to ARPANSA and abide by the other licence terms. The works are to be attributed to the Commonwealth as follows:-

‘© Commonwealth of Australia 2017, as represented by the Australian Radiation Protection and Nuclear Safety Agency (ARPANSA)’

The publication should be attributed as: *Establishing radiation qualities in radiation (RQR), radiation qualities based on aluminium added filter (RQA) and radiation qualities based on copper added filter (RQT) beams*.

Use of the Coat of Arms

The terms under which the Coat of Arms can be used are detailed on the Department of the Prime Minister and Cabinet website (www.dpmc.gov.au/government/commonwealth-coat-arms).

Enquiries regarding the licence and any use of this report are welcome.

ARPANSA
619 Lower Plenty Road
YALLAMBIE VIC 3085
Tel: 1800 022 333 (Freecall) or +61 3 9433 2211

Email: info@arpansa.gov.au
Website: www.arpansa.gov.au

Contents

Executive Summary	v
1. Introduction	1
2. Method	2
2.1 Unfiltered beam.....	4
2.2 RQR beams	4
2.2.1 Justification for 3% termination criterion	5
2.3 RQA beams	6
2.4 RQT beams.....	6
2.5 Transit time.....	7
2.6 Comparison with PTW	7
2.6.1 75 cm³ Pancake chamber	8
2.6.2 Nomex R/F detector	8
2.7 Uncertainty	9
3. Results	10
3.1 Unfiltered beam.....	10
3.2 RQR beams	11
3.3 RQA beams	12
3.4 RQT beams.....	14
3.5 Correction factors.....	17
3.6 Transit time.....	18
3.7 Comparison with PTW	20
3.7.1 75 cm³ Pancake chamber	20
3.7.2 Nomex R/F detector	21
3.8 Uncertainty	22
3.8.1 Calculation of beam uniformity correction factor	24
Appendix 1. Beam profile measurement	25
Appendix 2. Monitor chamber energy dependence	27

A2.1.	Monitor transmission	27
A2.2.	Monitor wall energy dependence	27
Appendix 3.	Aperture misalignment	29
Appendix 4.	Monitor chamber charge-collection voltage.....	31
Appendix 5.	Monitor Physical Calculations.....	32
A5.1.	Wall thickness.....	32
A5.2.	Monitor chamber field size calculation	33
Appendix 6.	Equipment specifications	34
Glossary.....	35
References.....	36

Executive Summary

In 2018, the Australian Radiation Protection and Nuclear Safety Agency (ARPANSA) established the radiation qualities in radiation (RQR), radiation qualities based on aluminium added filter (RQA) and radiation qualities based on copper added filter (RQT) beam qualities, as specified by the International Electrotechnical Commission (IEC) and International Atomic Energy Agency (IAEA). The new beam qualities were developed to provide a traceable standard in Australia for radiation dosimetry in diagnostic radiology, and also address existing deficiencies in this area.

This report documents the process and the results undertaken in 2018 to establish these beam qualities.

The three beam series were commissioned for a new dosimetry grade X-ray system. This system is also used to provide radiotherapy calibrations using the Physikalisch-Technische Bundesanstalt (PTB) TH Series of beam qualities and protection-level calibrations using the ISO 4037 wide and narrow series X-rays in the range of accelerating potentials from 40 kV_p to 320 kV_p.

[IEC 61267](#) *Medical Diagnostic X-ray Equipment — Radiation Conditions for Use in the Determination of Characteristics* and [IAEA TRS457](#) *Dosimetry in Diagnostic Radiology: An International Code of Practice* specify the first half-value layer (HVL) for the RQR, RQA and RQT series of beams and homogeneity for the RQR beam series. When comparing these two specifications, the maximum first HVL deviation is 1.7%, 4.4% and 1.0% for RQR, RQA and RQT series of beams. In addition, for RQR beam quality, the maximum homogeneity deviation is 0.02. These results show that the RQR, RQA and RQT series of beams commissioned by ARPANSA are well within IEC and IAEA specifications.

To evaluate the calibration capability of this system, a 75 cm³ pancake ion chamber and a R/F semiconductor detector were calibrated using the RQR and RQA series of beams, and then compared with the calibration performed by PTW-Freiburg, traceable to the German dosimetry standards at PTB. For the 75 cm³ chamber, the calibration coefficient deviations are within 1.2% and 1.3% for the RQR and RQA series of beams. For the semiconductor detector, the calibration coefficient deviations are within 0.2% for the RQR series of beams. For the semiconductor detector, there is no comparison of RQA data with that from PTW, as the calibration coefficients for RQA series of beams are not available. The calibration capability for the RQT series of beams has not been verified, as the X-ray mask necessary for the calibration was not available at the time of writing this report, which was 21 February 2018.

The uncertainty in the ARPANSA calibration coefficients is estimated to be 1.2% at k=2 for both RQR and RQA beam qualities. The laboratory is now able to provide calibration services for radiation detectors used in general X-ray radiography.

1. Introduction

In Australia, the largest contributor to population dose is medical radiation [1]. International bodies and medical physics organisations have devised quality assurance (QA) programmes [2-3] and test methodologies [4-5] for different imaging modalities and adjunct equipment. This is to ensure that radiological equipment is in optimal condition, such that diagnostic information is obtained at minimal radiation dose. Accurate radiation dosimetry underpins these tests.

The Australian Radiation Protection and Nuclear Safety Agency (ARPANSA) has published national diagnostic reference levels (NDRLs) for computed tomography [6]. These NDRLs act as a benchmark to ensure the radiation dose delivered for a particular procedure is not excessive. The setting of NDRLs relies on uniform traceable and accurate dosimetry measurements across the nation.

Dosimetry is also important in the investigation of radiation incidents in diagnostic and interventional radiology and in assessments of risk. Medical research involving ionising radiation exposures of human volunteers requires a report on the associated doses from a medical physicist [7]. These assessments are ultimately traceable to a dosimeter, which must be calibrated.

Dosimeter calibrations are performed by Secondary Standard Dosimetry Laboratories (SSDL) and Primary Standard Dosimetry Laboratories (PSDL). These laboratories demonstrate their equivalence through international comparisons arranged via the Bureau International des Poids et Mesures (BIPM), under the Comité International des Poids et Mesures Mutual Recognition Arrangement (CIPM MRA).

Radiation dosimetry in diagnostic radiology uses different radiation detectors for different imaging modalities. During the calibration of a dosimeter, it is necessary to use X-ray beam conditions that are relevant to the clinical applications. The International Electrotechnical Commission (IEC) has published beam qualities [8] to address the range of beam qualities needed in different clinical conditions. These beam qualities are adopted by the International Atomic Energy Agency (IAEA) in their diagnostic radiology dosimetry code of practice TRS-457 [9]. In general radiography (and limited applications in fluoroscopy and interventional procedures), the RQR series mimics typical X-ray beams incident on a patient while the RQA series simulates beams attenuated by a patient.

Although radiation dosimetry has been well established in radiotherapy, the same is not always true for diagnostic radiology. There has been recent international interest to address this worldwide deficiency [10-14]. Responding to the considerations outlined above, in 2018 ARPANSA established the RQR, RQA and RQT beam qualities as specified by the IEC and IAEA [8,9], to provide a traceable standard in Australia for radiation dosimetry in diagnostic radiology.

This report was developed to document the process and the results to establish these beam qualities in 2018. The new beams were commissioned on a new dosimetry grade X-ray system, which is also used to provide radiotherapy calibrations using the PTB TH Series of beam qualities [15] and protection-level calibrations using the ISO 4037 wide and narrow series X-rays [16-18] in the range of accelerating potentials from 40 kV_p to 320 kV_p.

We present a novel method for establishing the added filtration necessary to produce the IEC half-value layers (HVLs). Traceability for air kerma is provided directly by the Australian primary standard medium energy free-air chamber (MEFAC), which was also used for the determination of HVL and inherent filtration.

The majority of this report, together with some scientific investigation results, were published in the *Australasian Physical & Engineering Sciences in Medicine* journal as, 'Establishing IAEA TRS-457 Diagnostic X-ray Beam Qualities at the Australian Primary Standard Dosimetry Laboratory' [19].

2. Method

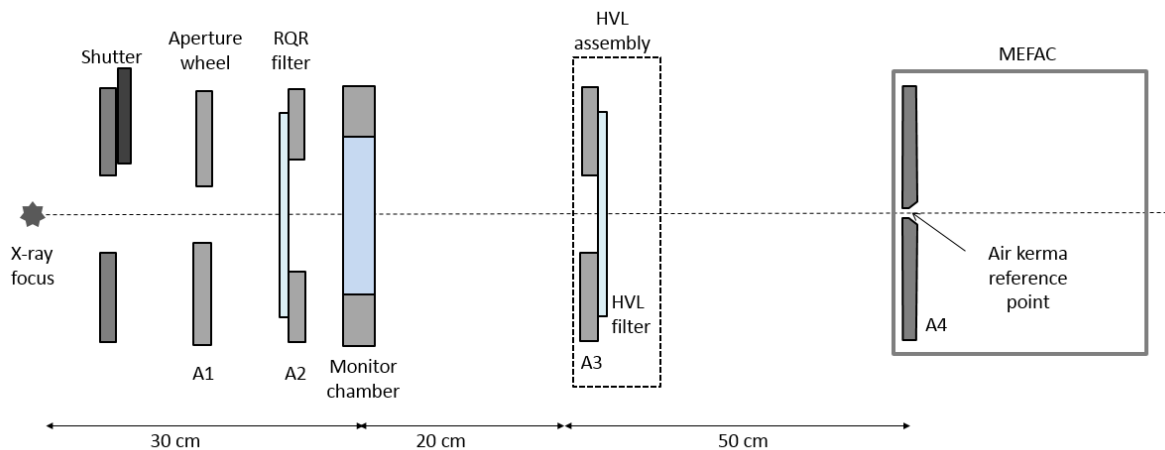


Figure 1 – Setup diagram

The experimental setup is shown in Figure 1. The X-ray focus to air kerma reference point distance (i.e., the measurement point) is 1 metre. In Figure 1, A1 is the aperture for defining the radiation field, A2 is the RQR filter exit-side aperture and additional filter holder, A3 is the HVL filter entrance-side aperture and A4 is the 5 mm diameter aperture for the MEFAC. The aperture wheel A1 consists of ten positions, evenly distributed on an aluminium disc of thickness 15.9 millimetre (mm). Each of these positions is fitted with a puck made of lead-antimony alloy. The dimensions of this puck are detailed in Figure 2. An aluminium ring with inner diameter 63.5 mm is fitted over the puck. Diameter A in Figure 2 varies with actual aperture size. The values are 1 to 6 centimetres (cm).

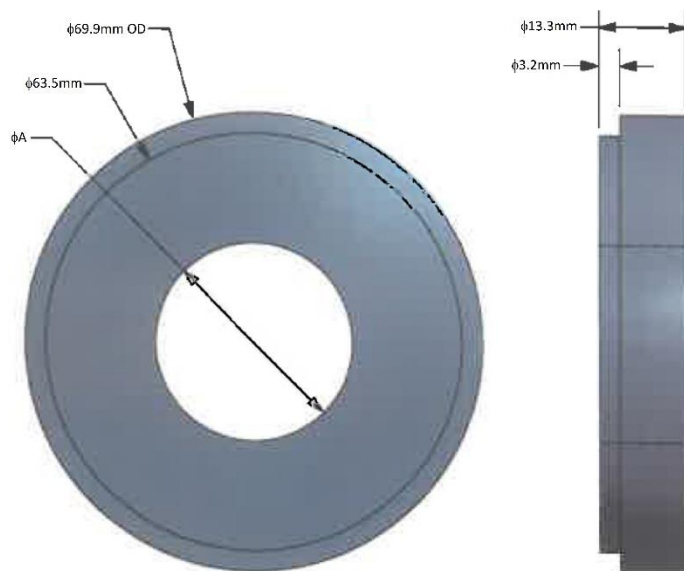


Figure 2 – Aperture puck

For realising the RQA beam qualities, additional filters as specified in TRS-457 [9] were manually added close to (but after) the aperture A2 using the additional filter holder. The HVL assembly was present only during attenuation curve measurements. During the monitor chamber calibrations and attenuation curve measurements, an in-house Labview program and Excel spreadsheet were used for equipment control, data collection and data analysis.

During attenuation curve measurements, the aperture A1 was set to a 2 cm diameter, which gave a nominal beam size of 10 cm in diameter at 1 m. The monitor chamber was calibrated for aperture A1 settings of 1 cm, 2 cm and 3 cm (for nominal field sizes of 5 cm, 10 cm and 15 cm at 1 m), so as to enable any of these aperture settings to be used during user detector calibration. The monitor chamber was calibrated in terms of the air kerma at the position of the MEFAC. The aperture of the MEFAC is 5 mm in diameter and this measures the central axis air kerma. Currents from the monitor chamber and MEFAC were measured simultaneously using two electrometers.

During calibration of the user detector, the MEFAC was replaced with the user detector and a known air kerma delivered. The centre of the active volume of the user detector was aligned to the test point. In this calibration, A1 was set to 3 cm in order to fully cover the 75 cm³ ionisation chamber (active diameter 91.4 mm [20]). The 75 cm³ ionisation chamber was connected to the PTW Nomex dosimeter T11050. To fully investigate the calibration capability of the ARPANSA system, two instrument settings for the 75 cm³ ionisation chamber were employed; one using accumulated charge over a period of 20 s and the other using air kerma. An Excel spreadsheet was developed for data collection and analysis.

The temperature, pressure, humidity, electron loss, scatter, fluorescence, aperture transmission and MEFAC air attenuation correction factors were applied during the monitor chamber calibration. The temperature, pressure and humidity correction factors for the MEFAC and the monitor chamber were obtained from real-time temperature, pressure and humidity measurements. Three thermistors were used to measure the temperature at the monitor, MEFAC and user chamber positions. The air attenuation factor was measured and other correction factors for the MEFAC were obtained by Monte

Carlo simulation in a previous study [21]. The saturation, chamber wall transmission and field distortion correction factors were all assumed to be unity.

2.1 Unfiltered beam

The steps for measuring the unattenuated beam were as follows:

1. Measure MEFAC and monitor chamber leakage (i.e., background value).
2. Using the existing HVL spreadsheet and for each RQR beam energy, the monitor and MEFAC currents were measured for different added filtration.
3. The ratio of the background-corrected MEFAC and monitor currents were calculated. This ratio is proportional to the transmission factor (TF).
4. The value of the lowest TF was confirmed to be $\leq 1/6$ of the unattenuated TF.
5. For each tube potential (40kV, 50kV, 60kV, 70kV, 80kV, 90kV, 100kV, 120kV, 150kV), a graph of TF vs filtration was plotted.
6. For each tube potential, the first HVL and second HVL were estimated from the attenuation curve.

2.2 RQR beams

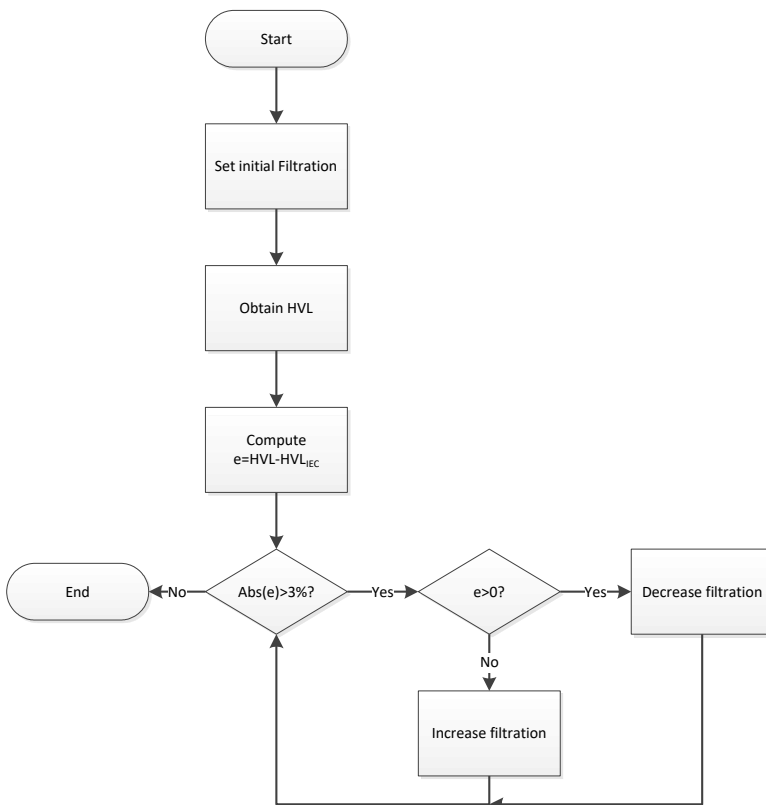


Figure 3 – Flowchart for beam filtration iteration. Abs() represents the absolute function.

The steps for achieving the RQR beam qualities were as follows:

- Following the steps as per TRS457 [9], a template was constructed for each RQR beam energy. The template was constructed on a transparent projector slide.

- Using the sliding template method (mentioned in TRS457 [9]), the required added filtration was determined for each beam energy.
- These required added filtrations formed the initial added filtration in the iterative process detailed below.
- Using a novel iterative process (see Figure 3), the required added-filtration for each RQR beam was determined as per the specifications in IEC 61267 [8]. The new filtration of each step is given by:

$$NewFiltration = CurrentFiltration + \left(\frac{HVL_{IEC} - HVL}{2} \right) \quad (1)$$

- The attenuation curves for each RQR beam were plotted.
- The first and second HVLs for each RQR beam were determined from the attenuation curve.
- Homogeneity coefficient for each RQR beam was computed using the equation

$$Homogeneity = \frac{First\ HVL}{Second\ HVL} \quad (2)$$

- Worst case iteration steps totalled eleven for RQR2 to achieve the termination condition. Further iterations were undertaken to achieve first HVL difference better than 3% (see section 3.2).

2.2.1 Justification for 3% termination criterion

Although IEC and IAEA specified that the transmission factor (TF) has to be in the range 0.485 – 0.515, the current setup at ARPANSA is more convenient for a direct comparison of HVLs. This is because ARPANSA already has a spreadsheet and Labview program for measuring HVL, whereas the IEC and IAEA method involves changing the filtration at the RQR wheel, which is not as convenient.

For a given attenuation curve plotted on linear-log XY axes, a line segment joining the points (x, 0.515) and (HVL, 0.5) has slope m given by:

$$\frac{\ln(0.515) - \ln(0.5)}{x - HVL} = m$$

Therefore, the allowable HVL range (x – HVL) is:

$$x - HVL = \ln(0.515) - \ln(0.5), \text{ for } m = 1$$

Hence:

$$x - HVL < \frac{\ln(0.515) - \ln(0.5)}{m}, \forall |m| > 1$$

If using 3% of specified HVL, this implies $x = HVL \times 0.97 = 1.377 \text{ mmAl}$. Hence, $m_{3\%} = -0.694$. Therefore it can be established that, as long as the polyenergetic beam slope magnitude ($|m_{poly}|$) is less than $|m_{3\%}|$, the allowable range using 3% of specified HVL will be smaller than the allowable range of the polyenergetic beam. This has been confirmed from measurements of the RQR 2 attenuation curve (worst case) which equals -0.461. For reference, the slope of a monoenergetic RQR 2 beam is $m_{mono} = -\ln(2)/HVL = -\ln(2)/1.42 = -0.488$.

2.3 RQA beams

The steps for achieving the RQA beam qualities were as follows:

- Filter preparation: Each aluminium filter to be added was measured at eight locations around the filter disc (see Table 6). The average thickness was determined. The filter was then numbered.
- Starting from the RQR beam, aluminium filtrations were added as per the thickness prescribed in IEC 61267 [8]. The iterative process mentioned in section 2.2 is unnecessary because the first HVLs specified in IEC 61267 are nominal values [8] if the RQA beams are implemented from RQR beams.
- The attenuation curves for each RQA beam were plotted.
- The first and second HVLs for each RQA beam were determined from the attenuation curve.

2.4 RQT beams

Using the copper filtrations suggested by IAEA TRS-457 [9], a trial and error process was used to achieve the RQT beam quality required by IEC 61267 [8] and IAEA TRS-457 [9]. The iterative process mentioned in section 2.2 cannot be used because the filtration material is copper, however the specified HVL is in mm Al. For each RQT beam, the transmission factor was:

1. Put the RQR filtration and the copper filter as suggested by IAEA TRS-457 [9] into the filter wheel slot.
2. After inserting all the aluminium and copper filters for all RQT beams, mount the filter wheel onto the Hopewell X-ray equipment.
3. Set the MEFAC so that it is 1 m from the focus.
4. Perform sixty background measurements using Labview script and find out the average leakage current from the MEFAC electrometer.
5. Set the tube voltage to the one of those specified by IAEA TRS-457 [9] for the RQT beam under test and tube current to 20 mA.
6. Perform twelve measurements using Labview script.
7. Copy the readings from the Labview generated CSV file to a spreadsheet.
8. Find the background-corrected readings for the MEFAC current for each of the twelve readings. These will be the unfiltered readings.
9. Form a stack aluminium filters with a total thickness equal to the HVL specified by IAEA TRS-457 [9] for the RQT beam under test. Need to measure (or recall if measured previously) individual filter thickness.
10. Put the stack of aluminium filter into the additional filter holder.
11. Perform twelve measurements using Labview script.
12. Copy the readings from the Labview generated CSV file to a spreadsheet.
13. Find the background-corrected readings for the MEFAC current for each of the twelve readings. These will be the filtered readings.

14. The transmission factor is the ratio of each background-corrected filtered readings to background-corrected unfiltered readings.
15. Find the average of these twelve transmission factors.
16. If the average transmission factor is between 0.485 to 0.515, then the beam has met the HVL condition as specified by IAEA TRS-457 [9].
17. Repeat steps 5 to 16 for all other RQT beams.

2.5 Transit time

X-ray exposures were controlled by a pneumatically actuated tungsten shutter. The transit time (τ) was measured by taking a long exposure (K_L) with exposure time (t) equal to 10 s followed by 10 (n) short exposures (K_n), each at 1 second (s) duration. The air kerma values for K_L and K_n were measured by the monitor chamber. The transit time was then calculated using the IAEA TRS-457 [9] transit time equation as follows:

$$\tau = t \frac{K_L - \sum_{n=1}^{10} K_n}{\sum_{n=1}^{10} K_n - 10K_L} \quad (3)$$

2.6 Comparison with PTW

The steps for calibrating the user detector were as follows:

- The monitor chamber is calibrated first to obtain the monitor chamber calibration coefficients (n_K). The MEFAC reference point (see Figure 1) was set at 1 m from the focus during this calibration.
- Based on previously published air kerma and measured charge relationship [22] (and assuming that bremsstrahlung escape is negligible), the calibration coefficient for the monitor chamber is then calculated using:

$$n_{K,Q} = \frac{|R_{ref,Q}| \times \prod_i k_{i,MEFAC}}{m_{air} \times \prod_i k_{i,monitor\ chamber}} \times \left(\frac{W}{e}\right) \quad (4)$$

where $R_{ref,Q}$ is the ratio of the reading of the MEFAC corrected for leakage and background to the reading of the monitor chamber corrected for leakage and background at beam quality Q.

k_i are the correction factors for the MEFAC and monitor chamber.

m_{air} is the mass of air inside the MEFAC measurement volume.

W/e is the mean energy required for an electron to produce an ion pair in dry air.

$n_{K,Q}$ is the calibration coefficient for the monitor chamber at beam quality Q.

- Owing to the way the measurements were performed (see sections 2.6.1 and 2.6.2), temperature, pressure and humidity will have to be captured manually from the TPH electronic file. The average values of temperature, pressure and humidity over the interval of measurement were used.
- Since the stability of the monitor chamber was verified by the on-going QA of the monitor chamber, the user detector was calibrated using the substitution method [9]. The user calibration coefficient is given by:

$$N_{K,Q}^{user} = \frac{n_{K,Q} \times M_Q^{ref}}{M_Q^{user}} \quad (5)$$

where $N_{K,Q}^{user}$ is the calibration coefficient for the user detector at beam quality Q

$M_{K,Q}^{ref}$ is the corrected reading of the monitor chamber at beam quality Q

$M_{K,Q}^{user}$ is the corrected reading of the user detector at beam quality Q

The correction factor (k_Q) is given by [9]:

$$k_Q = \frac{N_{K,Q}^{user}}{N_{K,Q_0}^{user}} \quad (6)$$

where N_{K,Q_0}^{user} is the calibration coefficient for the user detector at the reference beam quality. In line with the IAEA recommendation [9], the reference beam qualities were chosen as RQR5 or RQA5 in this study.

- Sixty background measurements were undertaken to account for the background reading and leakage. Both the monitor chamber electrometer and the user electrometer were set to low range.

2.6.1 75 cm³ Pancake chamber

The steps for calibrating the 75 cm³ pancake chamber were as follows:

- The MEFAC was replaced by the 75 cm³ chamber (PTW SFD chamber Type 34060, S/N 000317 [20]). The centre of the active volume of the pancake chamber was aligned to the reference point of the MEFAC so that it was 1 m from the X-ray focus.
- During calibration of the 75 cm³ ionisation chamber, the aperture A1 (see Figure 1) was set to 3 cm in order to fully cover the 75 cm³ ionisation chamber (active diameter 91.4 mm [20]).
- All the measurements mentioned below involved manually starting the monitor chamber electrometer, opening the shutter to let the exposure run for the preset 20 s duration and manually stopping the monitor chamber electrometer. Readings on both the monitor chamber electrometer and the Nomex electrometer (PTW Type 11050, S/N 130892 [23]) were recorded. Both electrometers were set to report charge accumulated. Air correction on the Nomex electrometer was disabled.
- Each beam quality took twelve measurements to complete. The tube current used was 10 mA and both electrometers were set to medium range.
- The spreadsheet 'General Calibration Spreadsheet No Auto Air Correction Reports Charge Spektr.xlsx' was used for data recording and analysis purposes.
- The spreadsheet calculated the 75 cm³ ionisation chamber calibration coefficients for each beam quality and compared them to the PTW results.

2.6.2 Nomex R/F detector

The steps for calibrating the R/F semiconductor detector (PTW Type T11049, S/N 101607 [23]) were as follows:

- The MEFAC was replaced by the R/F detector. The surface of the R/F detector was aligned to the reference point of the MEFAC.
- All the measurements below involved manually starting the monitor chamber electrometer, opening the shutter to let the exposure run for the preset 20 s duration and manually stopping the monitor chamber electrometer. Readings on both the monitor chamber electrometer and Nomex electrometer (PTW Type 11050, S/N 130892 [23]) were recorded. The monitor chamber electrometer was set to report charge accumulated while the Nomex electrometer was set to report kerma. Air correction on the Nomex electrometer was not applicable due to the type of detector used.
- During calibration of the R/F semiconductor detector, the aperture A1 (see Figure 1) was set to 2 cm in order to fully cover the active area of the R/F detector (largest dimension of the active area was 86 mm approximately [23]).
- Each beam quality took twelve measurements to complete. The tube current used was 20 mA and both electrometers were set to medium range.
- The spreadsheet ‘General Calibration Spreadsheet No Auto Air Correction 12Apr17.xlsx’ was used for data recording and analysis purposes.
- The spreadsheet calculated the R/F detector calibration coefficients for each beam quality and compared them to the PTW results.

2.7 Uncertainty

The steps for formulating the uncertainty budget were as follows:

- Uncertainty of the transit time was estimated by performing ten transit time measurements (see sections 2.5 and 3.6).
- Beam profile uncertainty was measured using the IBA Blue Phantom water tank with the Farmer dosimeter setup so that the long axis of the active volume was perpendicular to the X-ray beam (see Appendix 1).
- The physical constants, along with their relative standard uncertainties (u_i), applied to the MEFAC are listed in **Error! Reference source not found.**

Constant	Value	u_i (%)
Density of air	1.2047 kgm ⁻³	0.01 [24]
W_{air}/e	33.97 JC ⁻¹	0.35 [25]

Table 1 – Physical constants. Density of air is density of dry air at 293.15 K and 101.325 kPa.

- The uncertainty budget was formulated following the principles given in JCGM 100 [26].
- The uncertainties for the influencing quantities, namely electron loss, scatter, fluorescence, and aperture transmission were Type B uncertainties, given in [21] with coverage factors $k=1$. A fixed correction for air attenuation was used, even though this correction is influenced by the density of the air, and a standard uncertainty of 0.2% used to account for the effect changes in temperature and pressure have on air attenuation.

- For half-value layer measurements, the response of the MEFAC was not corrected for the different spectra (filtered and unfiltered). The worst-case uncertainty due to this spectral dependency is 0.5% at RQR2.

3. Results

3.1 Unfiltered beam

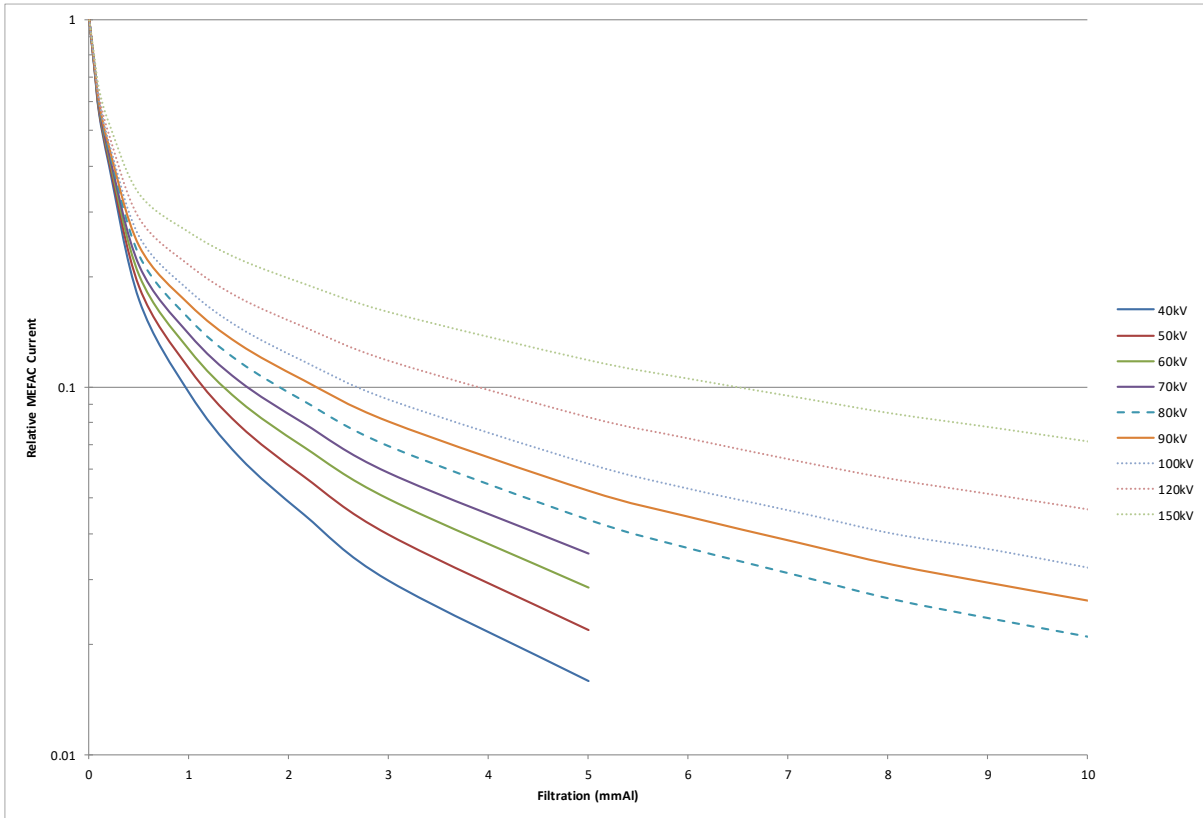


Figure 4 – Relative MEFAC current as a function of added aluminium from 40 kV to 150 kV. These curves reflect the inherent filtration of the X-ray tube.

Figure 4 shows the attenuation curves of the unfiltered X-ray tube at various tube voltages. The range of tube voltages in this figure corresponds to the range of tube voltages specified by the RQR2 to RQR10 beam qualities.

kV	Inherent HVL (mm Al)	Required first HVL (mm Al)	Required homogeneity coefficient	Width of window (mm Al)	Additional filtration (mm Al)
40	0.128	1.42	0.81	3.17	1.74
50	0.131	1.78	0.76	4.12	1.87
60	0.136	2.19	0.74	5.15	2.24
70	0.142	2.58	0.71	6.12	2.44
80	0.152	3.01	0.69	7.37	2.52
90	0.157	3.48	0.68	8.60	2.78
100	0.167	3.97	0.68	9.81	3.03
120	0.186	5.00	0.68	12.35	3.60
150	0.228	6.57	0.72	15.70	4.18

Table 2 – Beam characteristics, including the initial additional filtration as determined by the sliding template method. Required first HVL and homogeneity coefficients are values stipulated in IEC 61267 [8] and IAEA TRS-457 [9].

Table 2 lists the beam characteristics, including the initial additional filtration as determined by the sliding template method [8-9]. These additional filtrations were used as the initial filtration in our iterative algorithm. The inherent HVL column in Table 2 indicates the first HVL values of the inherent X-ray beams filtered by the tube assembly materials (e.g., cooling oil and beryllium window) between the X-ray focus and the tube exit port.

3.2 RQR beams

Figure 5 shows the RQR characteristics realised at ARPANSA. The beam quality parameters are listed in Table 4. The fourth column in Table 4 is the percentage difference of the measured first HVL when compared to the IEC-specified first HVL for RQR beams. The last column is the difference between the measured homogeneity coefficient and the IEC-specified homogeneity coefficient. Negative values in the fourth and last columns indicate that the measured value is less than the required value. IEC 61267 [8] and IAEA TRS-457 [9] require that the measured transmission factor has to be within 0.485 to 0.515 and the difference between the experimental homogeneity coefficient and the stipulated homogeneity coefficient is within 0.03.

	Filter Combination (mmAl)	Total Added Filtration (mmAl)
RQR2	2.03, 0.38	2.41
RQR3	2.0, 0.2, 0.2, 0.1	2.50
RQR4	2.02, 0.5	2.52
RQR5	2.85	2.85
RQR6	2.02, 0.97	2.99
RQR7	3.13	3.13
RQR8	2.14, 1.01, 0.1	3.25
RQR9	3.66, 0.1	3.76
RQR10	4.11, 0.2	4.31

Table 3 – List of filtrations used to realise the RQR beam qualities

	Added Filtration (mm Al)	First HVL (mm Al)	Difference to specified HVL (%)	Second HVL (mm Al)	Homogeneity coefficient	Difference to specified Homogeneity
RQR2	2.41	1.41	-0.7	1.79	0.79	-0.02
RQR3	2.50	1.81	1.7	2.42	0.75	-0.01
RQR4	2.52	2.16	-1.4	2.92	0.74	-0.00
RQR5	2.85	2.62	1.6	3.73	0.70	-0.01
RQR6	3.13	3.00	-0.3	4.45	0.67	-0.02
RQR7	3.36	3.52	1.2	5.19	0.68	-0.00
RQR8	3.48	3.92	-1.3	5.90	0.66	-0.02
RQR9	3.97	5.05	1.0	7.55	0.67	-0.01
RQR10	4.79	6.58	0.2	9.33	0.71	-0.01

Table 4 – List of RQR beam quality parameters

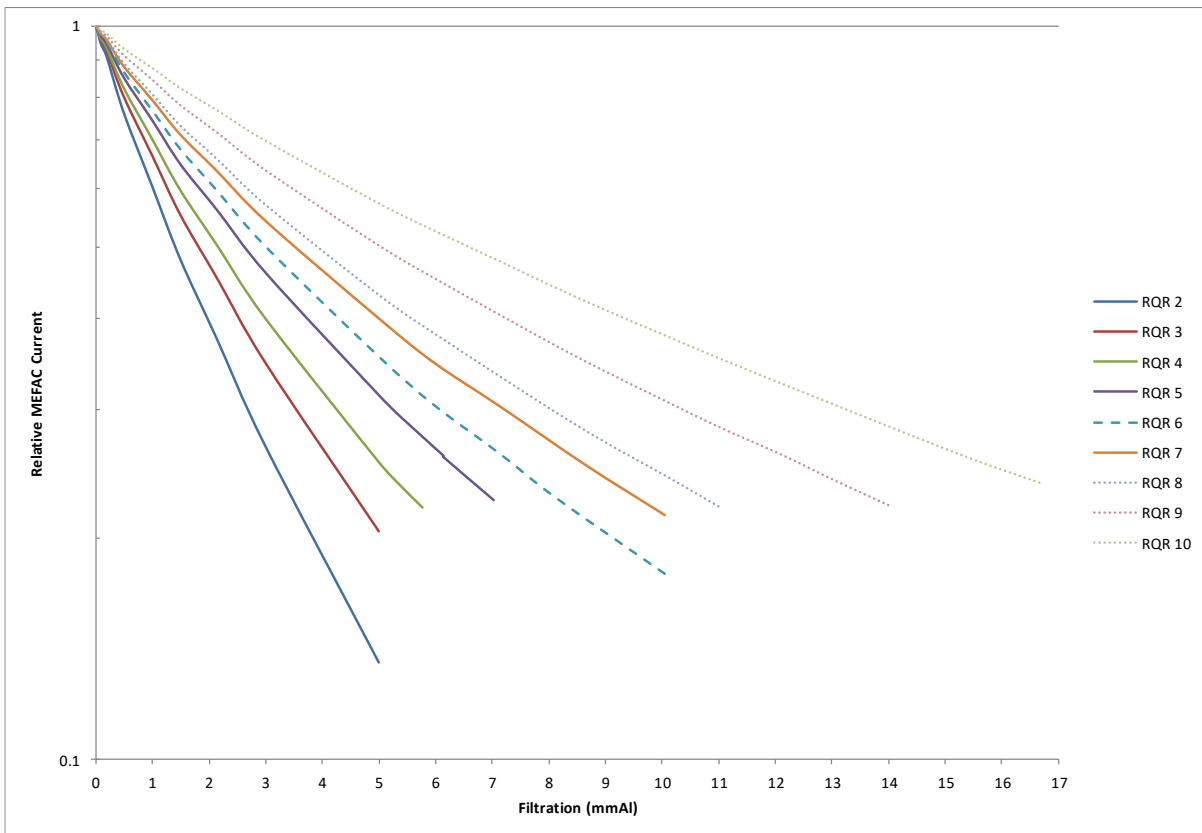


Figure 5 – Relative MEFAc current as a function of added aluminium for RQR beams

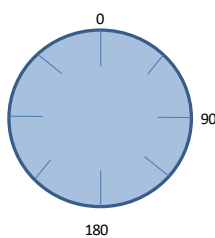
3.3 RQA beams

Table 5 lists the filter identification number and the total added filtration used to realise the RQA series of beams at ARPANSA. The total added filtration indicated in Table 5 excludes the RQR filtration. Table 6 shows the results of the filter thickness measurements for the added aluminium filters. Figure 6 shows the RQA beam characteristics realised at ARPANSA. The beam quality parameters are listed in Table 7.

	Filter Combination (mm Al)	Total Added Filtration (mm Al)
RQA2	COM148	4.00
RQA3	COM106	10.00
RQA4	COM106, 147, 148	16.02
RQA5	COM105, 106, 146	21.02
RQA6	COM105, 106, 147, 148	26.03
RQA7	COM104, 105, 106	30.02
RQA8	COM104, 105, 106, 148	34.02
RQA9	COM102, 104, 105, 106	40.02
RQA10	COM102, 104, 105, 106, 146, 148	45.03

Table 5 – List of filtrations used to realise the RQA beam qualities

COM	102	103	104	105	106	107	146	147	148	149	150	151	
Nominal Thickness	10	10	10	10	10	10	1	2	4	5	1	2	
Position	0	10.02	10.03	10.02	9.99	10.01	10.01	1.00	2.02	4.00	5.02	1.00	2.04
	45	10.01	10.01	10.01	10.01	10.01	10.01	1.00	2.02	4.00	5.02	0.99	2.03
	90	10.00	10.01	10.00	10.00	10.00	10.05	1.00	2.01	4.00	5.03	0.99	2.01
	135	10.00	10.03	10.00	10.00	10.00	10.06	1.03	2.02	4.00	5.02	1.06	2.00
	180	10.01	10.00	10.02	10.00	10.00	10.00	1.03	2.03	4.00	5.03	0.99	2.03
	225	10.00	10.00	10.00	10.01	10.01	10.03	0.99	2.02	4.00	5.02	0.99	2.09
	270	10.01	10.00	10.00	10.01	10.00	10.04	1.00	2.00	4.00	5.03	1.00	2.05
	315	10.01	10.02	10.00	10.02	10.00	10.00	1.00	2.00	4.01	5.02	1.02	2.11
Average		10.0075	10.0125	10.00625	10.005	10.00375	10.025	1.00625	2.015	4.00125	5.02375	1.005	2.045
SD		0.007071	0.012817	0.009161	0.009258201	0.005175	0.023299	0.015059	0.01069	0.003536	0.005175	0.024495	0.037796
C.V.		0.000707	0.00128	0.000916	0.000925357	0.000517	0.002324	0.014966	0.005305	0.000884	0.00103	0.024373	0.018482



0 = Thickness marking position

Table 6 – Measurements of filter thickness

	Total added filtration (mm Al)	First HVL (mm Al)	Difference to specified HVL (%)
RQA2	6.41	2.29	4.1
RQA3	12.50	3.89	2.4
RQA4	18.54	5.64	4.4
RQA5	23.87	7.03	3.4
RQA6	29.02	8.45	3.1
RQA7	33.15	9.46	2.8
RQA8	37.27	10.44	3.4
RQA9	43.78	12.08	4.1
RQA10	49.34	13.75	3.4

Table 7 – List of RQA beam quality parameters

The second column in Table 7 provides information about how the measured first HVL compares with the IEC specified first HVL for RQA beams. Since the IEC-specified first HVL values are nominal values, the percentage difference values are indicative only.

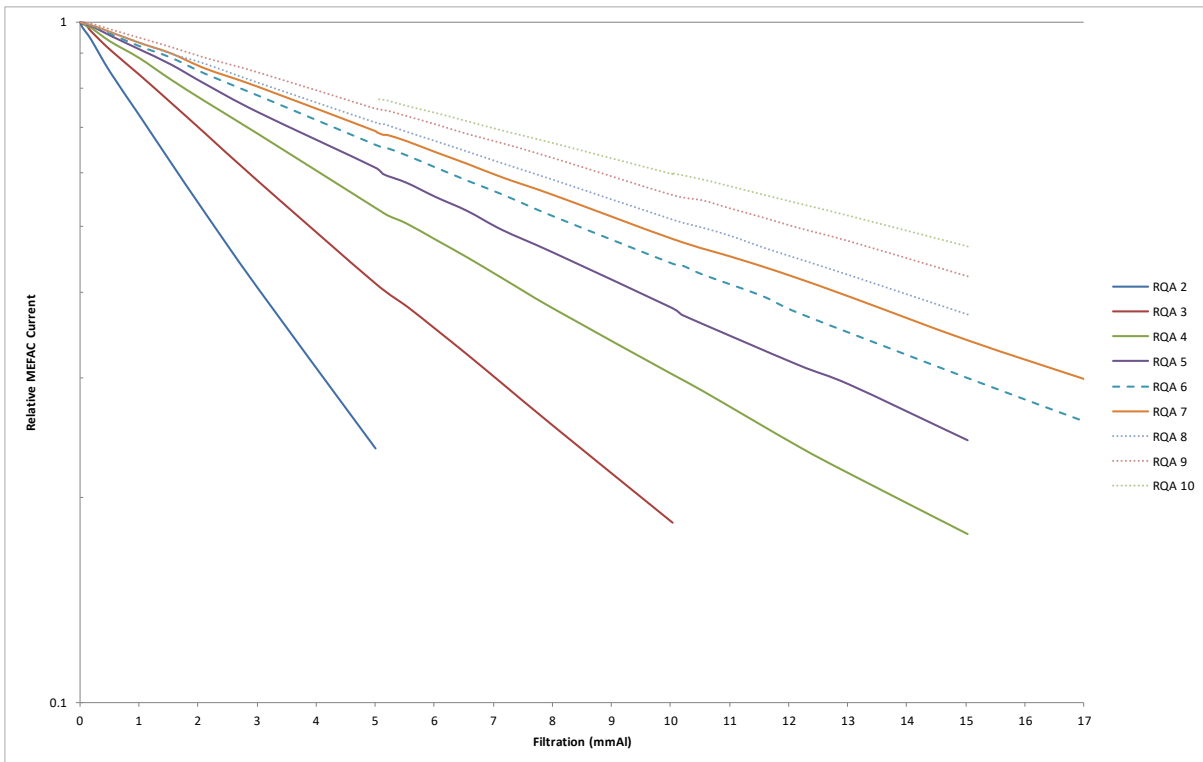


Figure 6 – Relative MEFAC current as a function of added aluminium for RQA beams

3.4 RQT beams

Table 8 lists the copper filter identification number and the total added copper filtration used to realise the RQT series of beams at ARPANSA. Note that the actual filtration will be the copper filtration plus the corresponding RQR filtration. Table 9 – List of RQT beam quality parameters

lists the RQT beam qualities achieved at ARPANSA.

	Filter Combination (mm Al)	Total Added Filtration (mm Cu)
RQT8	COM134, 140, 141, 142, 145	0.18
RQT9	COM130, 138	0.22
RQT10	COM131, 139	0.27

Table 8 – List of copper filtrations used to realise the RQT beam qualities

	First HVL (mm Al)	Difference to specified HVL (%)	Second HVL (mm Al)
RQT8	6.91	0.14	8.34
RQT9	8.55	1.79	10.03
RQT10	10.19	0.89	11.77

Table 9 – List of RQT beam quality parameters

	AI Filtration added (mm AI)	Average transmission factor
RQT8	6.91	0.501
RQT9	8.41	0.503
RQT10	10.07	0.501

Table 10 – Transmission factors for the RQT beams

The second column in Table 9 – List of RQT beam quality parameters

is the percentage difference of the measured first HVL when compared to the IEC-specified first HVL for RQT beams. A negative value indicates the measured first HVL is less than the required first HVL. Table 10 shows the transmission factors of the RQT beams. It can be seen that these factors lie within the IEC specified range of 0.485 – 0.515 [8].

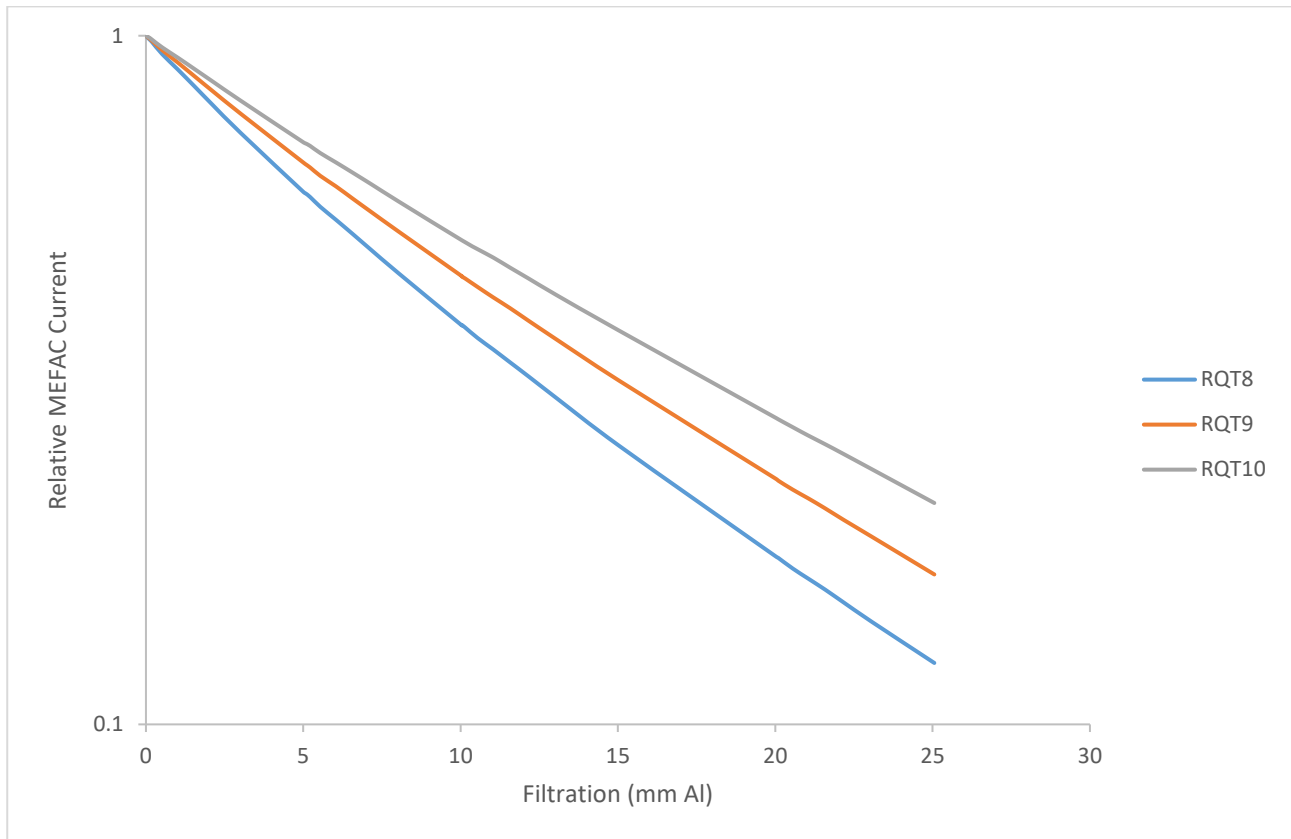


Figure 7 – Relative MEFAC current as a function of added aluminium for RQT beams

3.5 Correction factors

	Electron loss ke	Scatter ksc	Fluorescence kfl	Aperture transmission ktr	Air attenuation kair
RQR2	1.0001	0.9935	0.9974	0.9999	1.0198
RQR3	1.0001	0.9937	0.9976	0.9999	1.0169
RQR4	1.0001	0.9939	0.9978	0.9998	1.0153
RQR5	1.0001	0.9940	0.9980	0.9998	1.0135
RQR6	1.0001	0.9941	0.9982	0.9997	1.0125
RQR7	1.0001	0.9942	0.9983	0.9996	1.0116
RQR8	1.0001	0.9943	0.9984	0.9995	1.0108
RQR9	1.0003	0.9946	0.9986	0.9993	1.0095
RQR10	1.0007	0.9949	0.9989	0.9990	1.0083

Table 11 and Table 12 list the correction factors for the MEFAC for each of the RQR and RQA beam qualities. Not shown in these tables are the correction factors for density of air due to changes in

temperature, pressure and humidity conditions. The air density corrections are relative to reference conditions of 101.325 kPa and 20 °C.

	Electron loss k_e	Scatter k_{sc}	Fluorescence k_{fl}	Aperture transmission k_{tr}	Air attenuation k_{air}
RQR2	1.0001	0.9935	0.9974	0.9999	1.0198
RQR3	1.0001	0.9937	0.9976	0.9999	1.0169
RQR4	1.0001	0.9939	0.9978	0.9998	1.0153
RQR5	1.0001	0.9940	0.9980	0.9998	1.0135
RQR6	1.0001	0.9941	0.9982	0.9997	1.0125
RQR7	1.0001	0.9942	0.9983	0.9996	1.0116
RQR8	1.0001	0.9943	0.9984	0.9995	1.0108
RQR9	1.0003	0.9946	0.9986	0.9993	1.0095
RQR10	1.0007	0.9949	0.9989	0.9990	1.0083

Table 11 – Correction factors for the MEFAC for RQR beam qualities

These values were later revised in January 2022 – see TR 186.

	Electron loss k_e	Scatter k_{sc}	Fluorescence k_{fl}	Aperture transmission k_{tr}	Air attenuation k_{air}
RQA2	1.0001	0.9939	0.9978	0.9999	1.0139
RQA3	1.0002	0.9942	0.9980	0.9998	1.0101
RQA4	1.0002	0.9944	0.9985	0.9997	1.0085
RQA5	1.0002	0.9946	0.9988	0.9995	1.0077
RQA6	1.0002	0.9948	0.9991	0.9991	1.0071
RQA7	1.0002	0.9950	0.9993	0.9988	1.0068
RQA8	1.0002	0.9952	0.9994	0.9986	1.0065
RQA9	1.0006	0.9955	0.9996	0.9984	1.0062
RQA10	1.0022	0.9959	0.9997	0.9981	1.0058

Table 12 – Correction factors for the MEFAC for RQA beam qualities

These values were later revised in January 2022 – see TR 186.

3.6 Transit time

Table 13 shows the measurements for the shutter transit time. The transit time values are calculated using (3) in section 2.5 The transit time determination was repeated 10 times and the average transit time was 91.4 ms with a standard deviation of the mean of 0.21 % or 0.19 ms. For a typical exposure time of 20 s the impact of this uncertainty component is negligible.

Exposure	Charge (nC)	Nominal Exposure Time (s)									
1	236.5	236.4	236.5	236.6	236.5	236.6	236.5	236.6	236.6	236.5	10
2	25.53	25.63	25.60	25.58	25.64	25.56	25.54	25.65	25.63	25.53	1
3	25.64	25.54	25.51	25.55	25.54	25.56	25.58	25.64	25.62	25.61	1
4	25.50	25.51	25.54	25.58	25.54	25.62	25.54	25.68	25.58	25.56	1
5	25.57	25.53	25.53	25.61	25.55	25.65	25.57	25.54	25.53	25.64	1
6	25.62	25.62	25.66	25.60	25.62	25.63	25.62	25.56	25.61	25.54	1
7	25.57	25.59	25.65	25.62	25.58	25.65	25.61	25.54	25.63	25.63	1
8	25.61	25.52	25.51	25.57	25.55	25.66	25.54	25.58	25.52	25.57	1
9	25.51	25.54	25.54	25.54	25.55	25.64	25.62	25.53	25.65	25.56	1
10	25.57	25.55	25.52	25.59	25.60	25.57	25.56	25.69	25.69	25.58	1
11	25.53	25.52	25.55	25.63	25.65	25.56	25.56	25.60	25.56	25.59	1
Transit Time (ms)	90.79	90.83	90.59	91.32	91.60	92.42	91.22	91.99	92.04	91.55	

Table 13 – Transit time measurement

3.7 Comparison with PTW

3.7.1 75 cm³ Pancake chamber

	Monitor chamber	75 cm ³ Ion Chamber	PTW	Difference relative to PTW calibration	ARPANSA to PTW calibration coefficient ratio R	ARPANSA expanded uncertainty Uc (%)	PTW expanded uncertainty Uc (%)	Uncertainty of coefficient ratio U _R (%)
	$n_{K,Q}$ (Gy/C)	$N_{K,Q}^{user}$ (Gy/C)	$N_{K,Q}^{user}$ (Gy/C)	(%)				
RQR2	2.054×10 ⁵	3.725×10 ⁵	-	-	-	1.15	-	-
RQR3	1.909×10 ⁵	3.727×10 ⁵	3.767×10 ⁵	-1.1	0.989	1.15	2.5	2.75
RQR4	1.835×10 ⁵	3.730×10 ⁵	-	-	-	1.15	-	-
RQR5	1.757×10 ⁵	3.721×10 ⁵	3.767×10 ⁵	-1.2	0.988	1.15	2.5	2.75
RQR6	1.738×10 ⁵	3.732×10 ⁵	-	-	-	1.15	-	-
RQR7	1.716×10 ⁵	3.726×10 ⁵	3.767×10 ⁵	-1.1	0.989	1.15	2.5	2.75
RQR8	1.713×10 ⁵	3.730×10 ⁵	-	-	-	1.15	-	-
RQR9	1.700×10 ⁵	3.729×10 ⁵	3.767×10 ⁵	-1.0	0.990	1.15	2.5	2.75
RQR10	1.715×10 ⁵	3.717×10 ⁵	3.729×10 ⁵	-0.3	0.997	1.15	2.5	2.75

Table 14 – Calibration coefficients for the monitor chamber and a detector for RQR beam qualities. The calibration coefficients in both cases refer to the air kerma at 1 m in terms of the charge produced by that chamber for the 3cm aperture (nominal 15 cm beam at 1 m). See Error! Reference source not found. for ARPANSA uncertainty details.

	Monitor chamber	75 cm ³ Ion Chamber	PTW	Difference relative to PTW calibration	ARPANSA to PTW calibration coefficient ratio R	ARPANSA expanded uncertainty Uc (%)	PTW expanded uncertainty Uc (%)	Uncertainty of coefficient ratio U _R (%)
	$n_{K,Q}$ (Gy/C)	$N_{K,Q}^{user}$ (Gy/C)	$N_{K,Q}^{user}$ (Gy/C)	(%)				
RQA2	1.669×10 ⁵	3.727×10 ⁵	-	-	-	1.16	-	-
RQA3	1.266×10 ⁵	3.656×10 ⁵	3.705×10 ⁵	-1.3	0.987	1.16	2.5	2.76
RQA4	1.105×10 ⁵	3.676×10 ⁵	-	-	-	1.16	-	-
RQA5	1.034×10 ⁵	3.717×10 ⁵	3.742×10 ⁵	-0.7	0.993	1.16	2.5	2.76
RQA6	9.896×10 ⁴	3.738×10 ⁵	-	-	-	1.16	-	-
RQA7	9.602×10 ⁴	3.742×10 ⁵	3.742×10 ⁵	0.0	1.00	1.16	2.5	2.76
RQA8	9.259×10 ⁴	3.740×10 ⁵	-	-	-	1.16	-	-

RQA9	8.791×10 ⁴	3.734×10 ⁵	3.742×10 ⁵	-0.2	0.998	1.16	2.5	2.76
RQA10	8.611×10 ⁴	3.688×10 ⁵	3.667×10 ⁵	0.6	1.006	1.16	2.5	2.76

Table 15 – Calibration coefficients for the monitor chamber and a detector for RQA beam qualities. See Error! Reference source not found. for ARPANSA uncertainty details.

Table 14 lists the calibration coefficients for the monitor chamber and the user detector for each of the RQR beam qualities. Since the 75 cm³ ion chamber was previously calibrated by PTW, a comparison can be established by comparing the experimental calibration factor factors against the corresponding values in the calibration certificate supplied by PTW, traceable to German dosimetry standards at PTB (Physikalisch-Technische Bundesanstalt). Table 15 lists the calibration coefficients for the monitor chamber and the 75 cm³ ion chamber for each of the RQA beam qualities. It also lists the comparison with PTW calibration coefficients for the RQA beam qualities.

3.7.2 Nomex R/F detector

	Monitor chamber	R/F Detector correction factor	PTW	Difference relative to PTW calibration	ARPANSA to PTW calibration coefficient ratio R	ARPANSA expanded uncertainty Uc	PTW expanded uncertainty Uc	Uncertainty of coefficient ratio U _R
	$n_{K,Q}$ (Gy/C)	$N_{K,Q}^{user}$ (Gy/Gy)	$N_{K,Q}^{user}$ (Gy/Gy)	(%)		(%)	(%)	(%)
RQR2	4.589×10 ⁵	1.004	-	-	-	1.15	-	-
RQR3	4.262×10 ⁵	1.004	-	-	-	1.15	-	-
RQR4	4.091×10 ⁵	0.999	-	-	-	1.15	-	-
RQR5	3.920×10 ⁵	1.001	0.999	0.1	1.002	1.15	2.5	2.75
RQR6	3.874×10 ⁵	0.999	-	-	-	1.15	-	-
RQR7	3.827×10 ⁵	1.001	0.998	0.2	1.003	1.15	2.5	2.75
RQR8	3.817×10 ⁵	1.002	-	-	-	1.15	-	-
RQR9	3.789×10 ⁵	1.005	-	-	-	1.15	-	-
RQR10	3.819×10 ⁵	1.009	-	-	-	1.15	-	-

Table 16 – Calibration coefficients for the monitor chamber and the R/F detector for RQR beam qualities

	Monitor chamber $n_{K,Q}$ (Gy/C)	R/F Detector correction factor $N_{K,Q}^{user}$ (Gy/Gy)
RQA2	3.651×10^5	0.984
RQA3	2.811×10^5	0.994
RQA4	2.438×10^5	0.990
RQA5	2.271×10^5	0.998
RQA6	2.168×10^5	1.001
RQA7	2.099×10^5	0.994
RQA8	2.022×10^5	0.997
RQA9	1.936×10^5	0.995
RQA10	1.900×10^5	0.992

Table 17 – Calibration coefficients for the monitor chamber and the R/F detector for RQA beam qualities

Table 16 lists the calibration coefficients for the monitor chamber and the user detector for each of the RQR beam qualities. Since the R/F detector was previously calibrated by PTW, a comparison can be established by comparing the experimental calibration factor against the corresponding values in the calibration certificate supplied by PTW. The ARPANSA uncertainty in Table 16 is assumed to be the same as that used for the 75 cm³ pancake. In reality, this probably will overestimate the uncertainty slightly as the radiation field used in the R/F detector calibration is 2 cm, whereas the radiation field used in the pancake chamber calibration is 3 cm. Table 17 lists the calibration coefficients for the monitor chamber and the R/F detector for each of the RQA beam qualities. Since no calibration results were available from the PTW calibration certificate, comparisons of the ARPANSA calibration coefficients and the PTW calibration coefficients were not possible.

3.8 Uncertainty

Table 18 shows the uncertainty budget of the calibration system at ARPANSA. This budget was constructed by following the instructions given in JCGM 100 [26]. The combined relative expanded uncertainty is 1.15% with a coverage factor of 2 for RQR beam qualities and 1.16% with a coverage factor of 2 for RQA beam qualities. The uncertainties are discussed in detail in references [21] and [24].

Figure 10 shows the beam profile for the 3 cm aperture measured using the IBA Blue Phantom 2 3D scanning water tank and a Farmer-type chamber (PTW model 30013), mounted with its axis perpendicular to the beam. A correction for the non-uniform irradiation of the sensitive area (volume) of the PTW chamber of 1.0085 was derived from this data using a diameter of 91.4 mm [20].

Symbol	Quantity Name	Type A Standard Uncertainty (%)	Type B Standard Uncertainty (%)
k_a	MEFAC air attenuation		0.2 [24]
k_{sc}	MEFAC scattered radiation		0.04 [24]
k_{fl}	MEFAC fluorescence		0.03 [24]
k_e	MEFAC electron loss		0.02 [24]
k_s	MEFAC ion recombination		0.01 [24]
k_{pol}	MEFAC polarity		0.01 [24]
k_d	MEFAC field distortion		0.05 [24]
k_{tr}	MEFAC aperture transmission and scatter		0.06 [24]
k_h	MEFAC humidity		0.03 [24]
	Ionisation current ratio (MEFAC/Monitor)	0.025	
	Absolute calibration of MEFAC electrometer		0.15
	MEFAC volume		0.04
	MEFAC positioning		0.05
$(W/e)_{air}$	Physical constants		0.35 [25]
	MEFAC thermistor calibration		0.005
	Temperature uniformity in MEFAC		0.035
	MEFAC background		0.015
τ	Transit Time (for a 20 s exposure time)	0.002	
	User Instrument Resolution (for the 75 cm ³ Ion Chamber)		0.25
	Beam Uniformity		0.17*
	Positioning for User Instrument		0.2
	User Instrument Raw Reading RQR	0.019	
	User Instrument Raw Reading RQA	0.068	
	Combined relative expanded uncertainty RQR		1.15
	Combined relative expanded uncertainty RQA		1.16

Table 18 – Uncertainty budget of the calibration system. * A correction factor of 1.0085 was calculated for a 91.4 mm diameter active area, and the residual uncertainty is estimated to be 0.17%.

3.8.1 Calculation of beam uniformity correction factor

For $\pm 46\text{mm}$ (i.e. for a $\phi 92\text{mm}$ field), worst case deviation (averaged over 10 data points) = 97.5190 (H), 96.9190 (V), and $m = (98.1585 - 96.919) / (0 - 46) = -1.2395 / 46$ and $c = 98.1585$. Hence,

$$P(r) = -\frac{1.2395}{46}r + 98.1585$$

and

$$\int_0^{46} P(r)rdr = -\frac{1.2395}{46} \left| \frac{r^3}{3} \right|_0^{46} + 98.1585 \left| \frac{r^2}{2} \right|_0^{46} \quad (1)$$

$$= 103851.693 - 874.2607 = 102977.4323$$

$$\int_0^{46} P(0)rdr = 98.1585 \left| \frac{r^2}{2} \right|_0^{46}$$

$$= 103851.693$$

$$\frac{\int_0^{46} P(r)rdr}{\int_0^{46} P(0)rdr} = \frac{102977.4323}{103851.693} = 0.9916$$

Since profile at edge is less than profile at central axis, actual k_r is therefore $1/0.9916 = 1.0085$.

Appendix 1. Beam profile measurement

The IBA Blue Phantom water tank was setup as shown in the figures below. Care was taken to ensure that the scanning plane was orthogonal to the X-ray beam. Figure 8 shows the setup using the CC13 dosimeter and **Error! Reference source not found.** shows the setup using the Farmer dosimeter. Figure 10 shows the beam profile for the 3 cm aperture measured using the IBA Blue Phantom 2 3D scanning water tank and a Farmer-type chamber (PTW model 30013), mounted with its axis perpendicular to the beam.

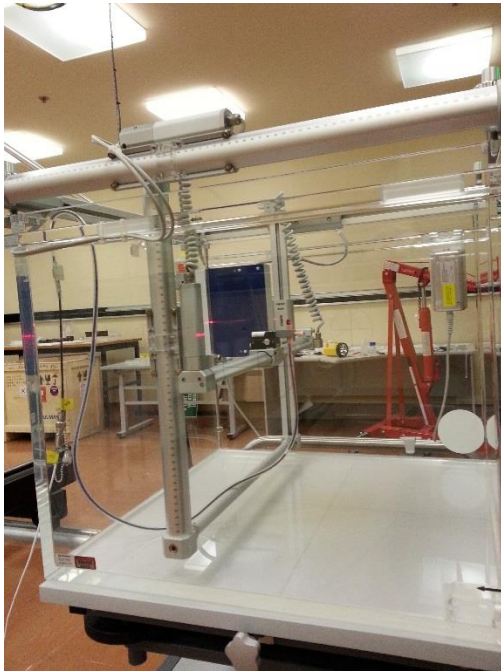


Figure 8 – CC13 chamber setup

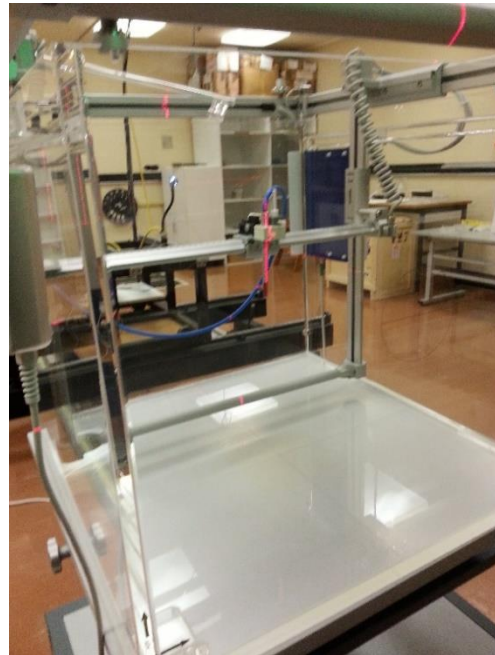


Figure 9 – Farmer chamber setup

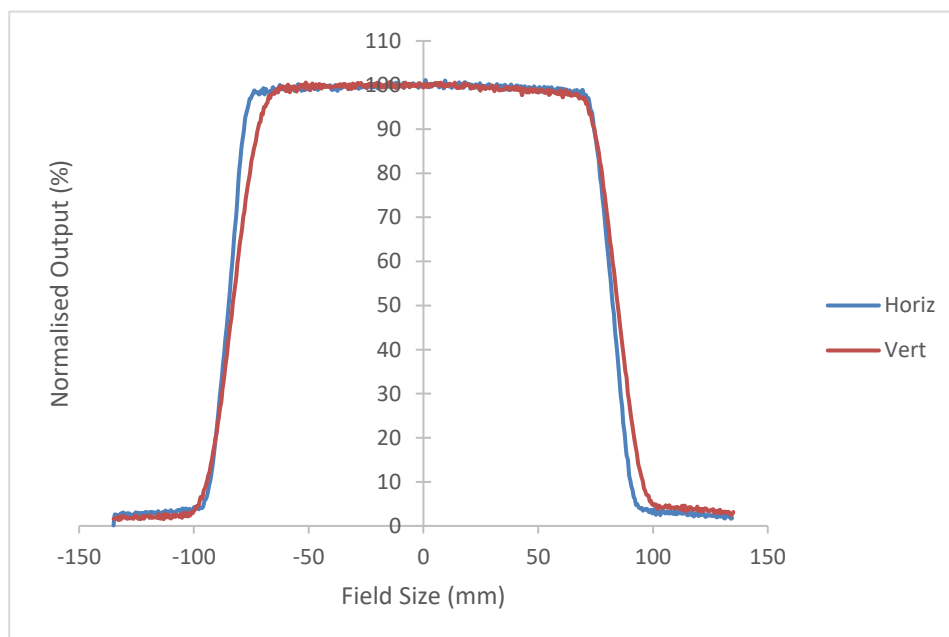


Figure 10 – Beam profile for RQR10 at 3 cm aperture measured using Farmer chamber

IAEA TRS-457 [9] requires that the beam profile variation is not more than 2% over an 80% field area about the central axis of the beam. For the 3 cm aperture, the radiation field size is nominally 150 mm and 80% about the central axis corresponds to ± 60 mm in Figure 10. From the beam profile data, the maximum deviation from the central kerma is 1.86% in the vertical direction. Hence the beam profile meets the IAEA TRS-457 beam profile requirement.

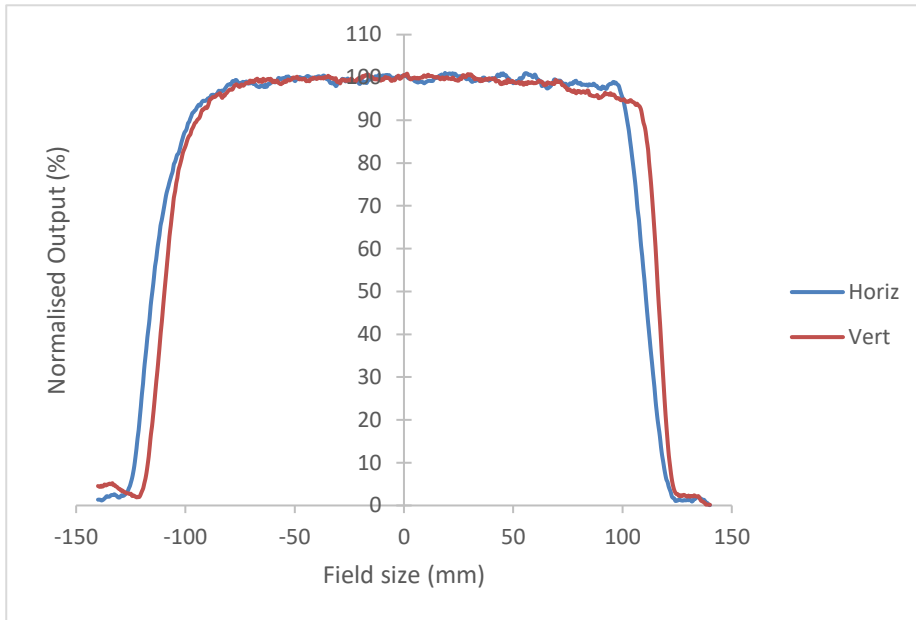


Figure 11 – Beam profile for RQR10 at 3cm aperture measured using CC13 chamber

Figure 11 shows the beam profile of RQR10 beam quality using 3 cm aperture measured using the CC13 chamber. This beam profile data was smoothed using a moving average filter of length 10.

Appendix 2. Monitor chamber energy dependence

A2.1. Monitor transmission

The MEFAC was placed at 1 m from the focus. X-ray beams of different tube potentials were projected to the MEFAC. The monitor chamber was moved out of the X-ray beam. This produced the unattenuated beam data. The experiment was repeated with the monitor chamber in its normal position. This produced the attenuated beam data. The ratio of the MEFAC current gives the transmission factor of the monitor chamber.

	1cm	2cm	3cm	4cm	5cm	6cm
RQR2	0.984894	0.982495	0.986455	0.984598	0.987029	0.985173
RQR3	0.986344	0.986123	0.986643	0.986288	0.987885	0.988181
RQR4	0.987062	0.987294	0.987191	0.987264	0.987953	0.987862
RQR5	0.98968	0.988196	0.989209	0.989274	0.989055	0.989277
RQR6	0.990429	0.988571	0.989039	0.989396	0.98976	0.989376
RQR7	0.992081	0.990237	0.989119	0.989363	0.989891	0.990799
RQR8	0.992156	0.990017	0.990504	0.99147	0.991173	0.990958
RQR9	0.992813	0.990962	0.99086	0.993205	0.991507	0.991929
RQR10	0.992411	0.991857	0.991146	0.99312	0.992735	0.991677

Table 19 – Monitor chamber transmission factor at various beam energy and aperture size

A2.2. Monitor wall energy dependence

The monitor wall and collecting electrodes are made of graphite-coated polyimide. The chemical formula for polyimide is $C_{22}H_{10}N_2O_5$ with a density of 1.42 g/cm^3 . Using Spektr 3.0 [27], the attenuation spectrum of polyimide was generated.

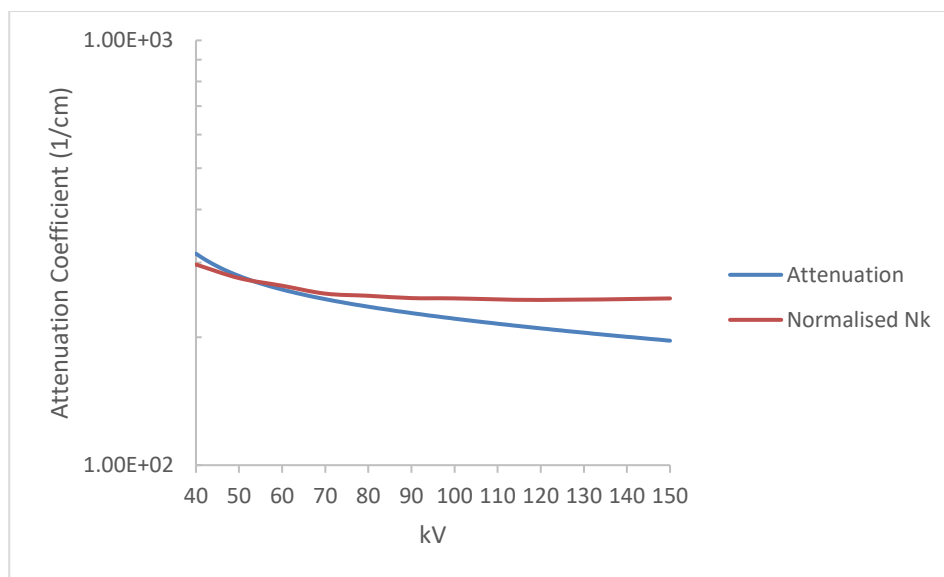


Figure 12 – Attenuation coefficient of polyimide and normalised N_k for monitor chamber

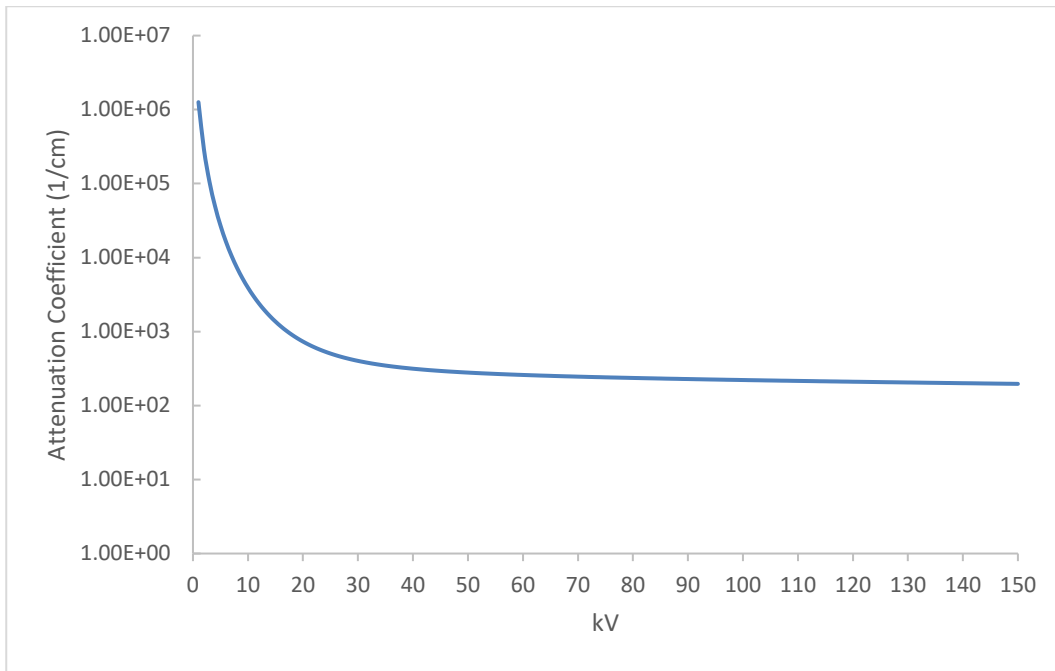


Figure 13 – Attenuation coefficient for polyimide over 0 kV to 150 kV

Appendix 3. Aperture misalignment

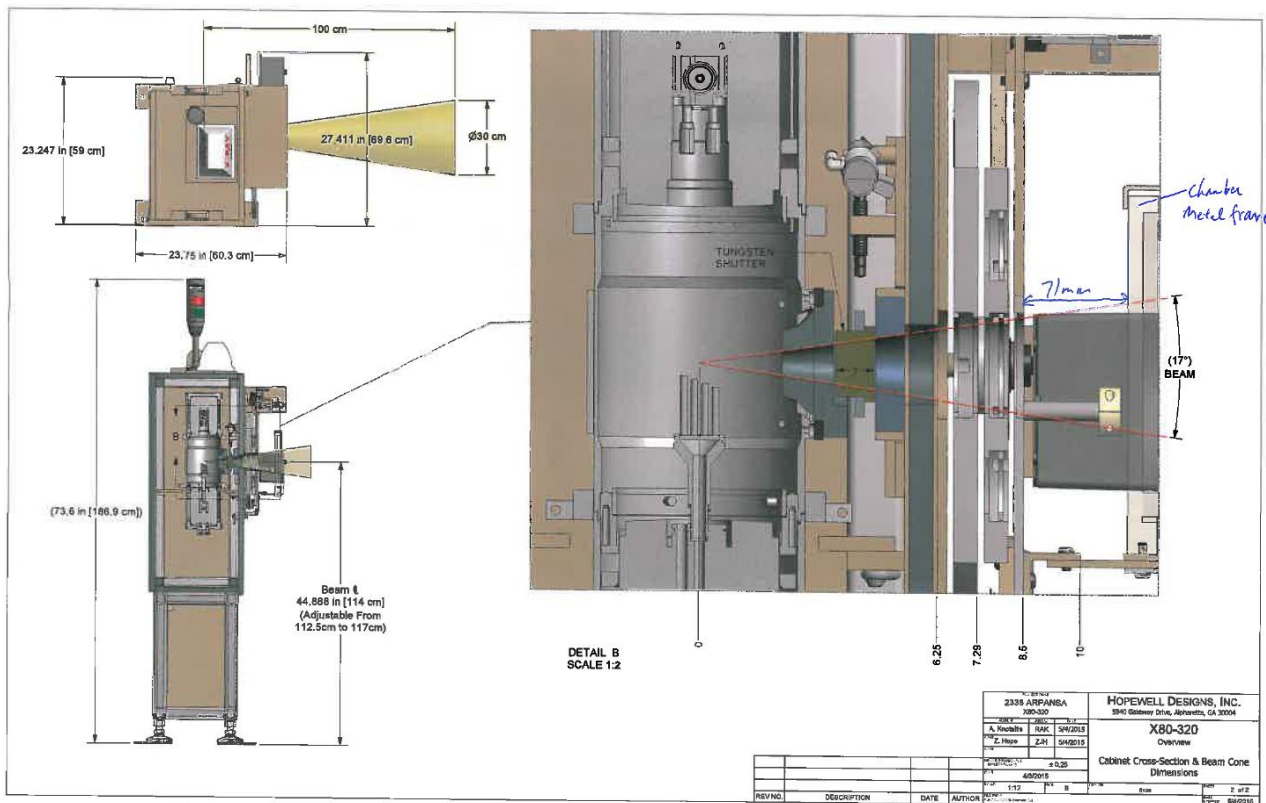


Figure 14 – Cabinet cross-section and beam cone dimensions

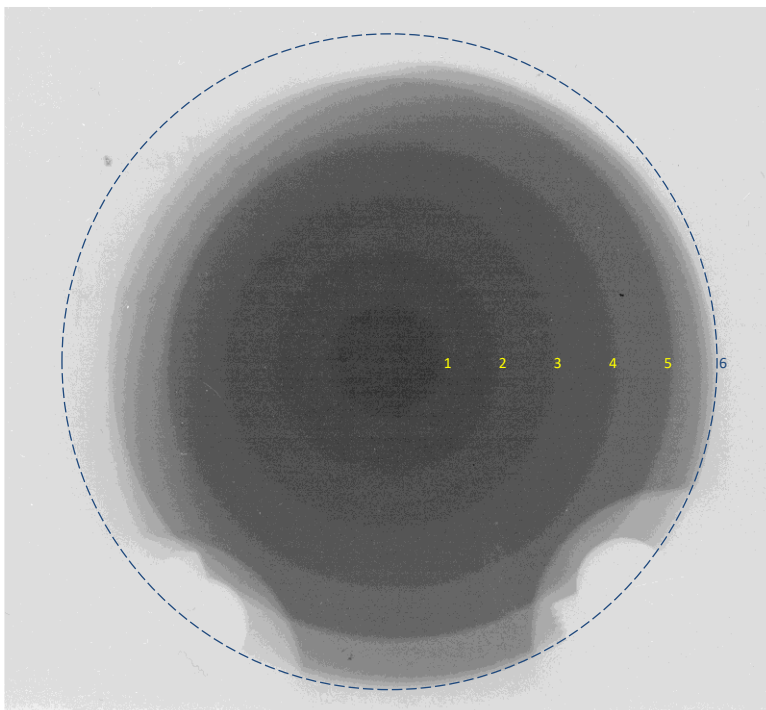


Figure 15 – X-ray fields for 1 cm to 6 cm aperture superimposed

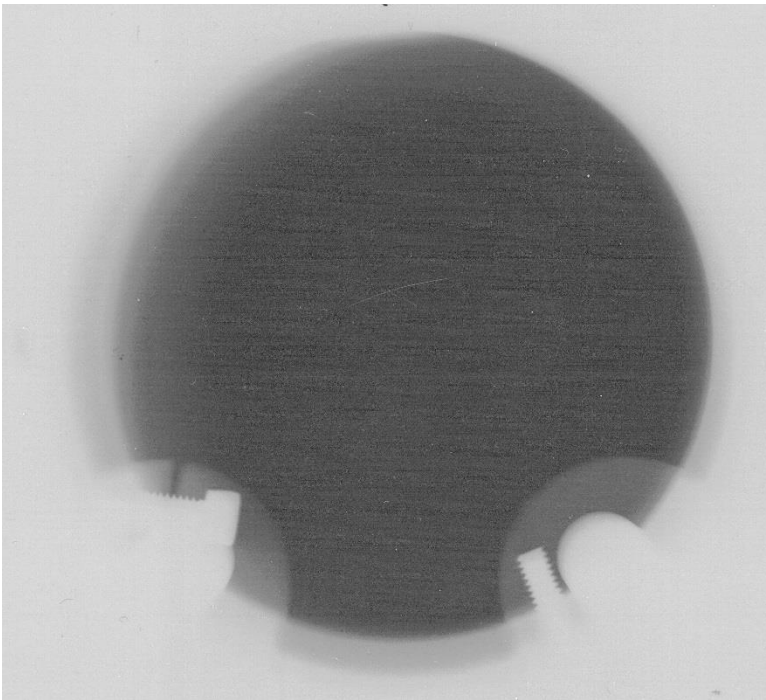


Figure 16 – X-ray fields for open aperture and 6 cm aperture superimposed

The 6 cm aperture has a radiation field diameter of 86 mm at the entrance surface of the monitor chamber. The active diameter of the monitor chamber is 148 mm, more than enough for the radiation field size. Figure 15 shows a film of the radiation fields for all aperture sizes superimposed. As can be seen from the figure, the radiation field for the 6 cm aperture is highly non-uniform. This is further demonstrated in Figure 16, where the region between the 9 o'clock position to 12 o'clock position was attenuated, due to a misalignment of the open aperture and the 6 cm aperture. This explains why the corresponding region in Figure 15 was missing. In addition, Figure 15 shows that the washers and part of the rails intruded into the radiation fields of the 5 cm and 6 cm aperture sizes. The intrusions of the washers and the rail into the large field sizes is also shown in the Cabinet cross-section and beam cone dimensions drawing (Figure 14).

Appendix 4. Monitor chamber charge-collection voltage

	Monitor $I_{ref}/Area$ (nAcm ⁻²)					
	1cm	2cm	3cm	4cm	5cm	6cm
RQR2	0.0615	0.0633	0.0629	0.0612	0.0541	0.0424
RQR3	0.1117	0.1150	0.1143	0.1113	0.0985	0.0772
RQR4	0.1719	0.1769	0.1758	0.1711	0.1515	0.1189
RQR5	0.2119	0.2179	0.2166	0.2109	0.1868	0.1467
RQR6	0.2706	0.2781	0.2766	0.2694	0.2388	0.1876
RQR7	0.3264	0.3353	0.3333	0.3246	0.2878	0.2260
RQR8	0.3920	0.4026	0.4003	0.3902	0.3460	0.2719
RQR9	0.4941	0.5071	0.5040	0.4911	0.4357	0.3425
RQR10	0.6779	0.6952	0.6908	0.6730	0.5974	0.4699

Table 20 – Normalised monitor chamber current at 200V collection voltage

	Monitor $I_{ref}/Area$ (nAcm ⁻²)					
	1cm	2cm	3cm	4cm	5cm	6cm
RQR2	0.0621	0.0640	0.0634	0.0619	0.0545	0.0429
RQR3	0.1128	0.1161	0.1153	0.1124	0.0992	0.0782
RQR4	0.1735	0.1785	0.1772	0.1728	0.1526	0.1204
RQR5	0.2138	0.2198	0.2183	0.2128	0.1881	0.1485
RQR6	0.2730	0.2807	0.2786	0.2718	0.2404	0.1901
RQR7	0.3291	0.3383	0.3358	0.3274	0.2897	0.2291
RQR8	0.3952	0.4060	0.4032	0.3934	0.3483	0.2756
RQR9	0.4977	0.5110	0.5075	0.4949	0.4381	0.3470
RQR10	0.6825	0.7001	0.6951	0.6776	0.6005	0.4759

Table 21 – Normalised monitor chamber current at 300V (default) collection voltage

	Monitor $I_{ref}/Area$ (nAcm ⁻²)					
	1cm	2cm	3cm	4cm	5cm	6cm
RQR2	0.0618	0.0635	0.0631	0.0614	0.0545	0.0424
RQR3	0.1122	0.1155	0.1147	0.1117	0.0992	0.0773
RQR4	0.1725	0.1775	0.1763	0.1717	0.1527	0.1190
RQR5	0.2127	0.2187	0.2173	0.2117	0.1884	0.1469
RQR6	0.2716	0.2791	0.2774	0.2703	0.2408	0.1879
RQR7	0.3275	0.3365	0.3343	0.3257	0.2901	0.2263
RQR8	0.3934	0.4040	0.4016	0.3916	0.3488	0.2724
RQR9	0.4958	0.5088	0.5056	0.4927	0.4390	0.3431
RQR10	0.6800	0.6974	0.6927	0.6750	0.6021	0.4708

Table 22 – Normalised monitor current at 400V collection voltage

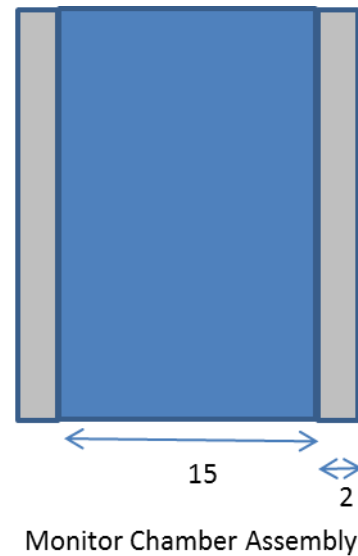
The high voltage supply to the monitor chamber was varied using the electrometer to investigate its effect on the monitor chamber current. These experiments were performed to determine if the charge-collection voltage caused the variation of normalised monitor chamber calibration coefficient across beam energy.

Appendix 5. Monitor Physical Calculations

A5.1. Wall thickness

Measurements		
Silver frame of monitor		
Opening diameter	160	mm
Silver frame outermost edge diameter	230	mm
Silver frame to monitor wall gap	1	mm
Silver frame thickness	2	mm
No. of silver frames	2	
Monitor thickness	15	mm

Filter holder		
Hole diameter		mm
Thickness	6	mm
Exit surface of filter holder to monitor frame	71	mm



Note the measured monitor thickness is very different to the calculated active thickness of 5mm.

Calculation		
Focus to monitor wall	286.9	mm
Focus to silver frame	283.9	mm
5cm aperture field at frame	70.975	mm
6cm aperture field at frame	84.85828	mm
Focus to filter holder entrance	209.9	mm
5cm aperture field at filter holder	52.475	mm
5cm aperture field at filter holder exit	53.975	mm
6cm aperture field at filter holder	62.73953	mm
6cm aperture field at frame holder exit	64.53294	mm

A5.2. Monitor chamber field size calculation

Aperture wheel diameter	380	mm
Aperture wheel diameter on drawing	123	mm
From aperture wheel drawing, scale of drawing is	3.089431	
Hence thickness of aperture wheel is	15.44715	mm

Using cabinet cross-section & beam cone dimension drawing

Focus to filter wall	215.9	mm
Filter wall to chamber metal frame	71	mm
Focus to monitor	286.9	mm

For 5cm aperture,

Field at 1m	250	mm
Half beam angle	7.125016	degree
Field at monitor is	71.725	mm

Which is smaller than 148mm

For 6cm aperture,

Field at 1m	300	mm
Half beam angle	8.5	degree
Field at monitor is	85.75498	mm

Which is smaller than 148mm

Appendix 6. Equipment specifications

The Hopewell X80-320-A X-Ray Irradiator System is a dosimetry grade system based on a Gulmay Comet MXR-320 tube. The system has the following specifications [20, 28-29]:

Item	Value	TRS-457 Requirement [9]
Electrometer offset current	$\leq \pm 1$ fA at 100 fA	<2% of the maximum indication in the most sensitive range
Digitisation resolution	1 fA	N/A
Monitor chamber leakage current	$\leq \pm 10$ fA	Below 10 fA for reference class chamber
Shutter material	25 mm tungsten	2 mm lead
Shutter Transit Time	85.70 ms	N/A
Tube port material	3 mm beryllium	<2.5 mm Al quality equivalent filtration
Target material	Tungsten	Tungsten
Anode angle	20°	$\leq 27^\circ$
Cooling	Oil-to-water cooler	Liquid cooled
Percentage Ripple	0.09% over 5m cable	<10%

Table 23 – List of vital equipment specifications

Glossary

CT

Computed tomography. See https://en.wikipedia.org/wiki/CT_scan.

KERMA

Kerma is an acronym for "kinetic energy released per unit mass". See [https://en.wikipedia.org/wiki/Kerma_\(physics\)](https://en.wikipedia.org/wiki/Kerma_(physics)).

HVL

Half-value layer. See https://en.wikipedia.org/wiki/Half-value_layer.

MEFAC

Medium energy free-air chamber. A primary standard at ARPANSA.

Transmission factor

The ratio of the exiting radiation to the incident radiation.

References

1. Australian Radiation Protection and Nuclear Safety Agency (ARPANSA), 2015. *Ionising Radiation and Health*, Fact sheet, Yallambie.
2. International Atomic Energy Agency (IAEA), 2012. *Quality Assurance Programme for Computed Tomography: Diagnostic and Therapy Applications*, IAEA Human Health Series No. 19, IAEA, Vienna
3. European Commission, 2012. *Cone Beam CT for Dental and Maxillofacial Radiology*, Radiation Protection No. 172
4. Lee KL, Ireland TA, Bernardo M, 2016. *Benchmarking the performance of fixed-image receptor digital radiography systems Part 1: a novel method for image quality analysis*, Australas Phys Eng Sci Med, 39:453, doi:10.1007/s13246-016-0440-3
5. Lee KL, Bernardo M, Ireland TA, 2016. *Benchmarking the performance of fixed-image receptor digital radiography systems. Part 2: system performance metric*, Australas Phys Eng Sci Med 39:463, doi:10.1007/s13246-016-0439-9
6. Hayton A, Wallace A, Marks P, Edmonds K, Tingey D, Johnston P, 2013. *Australian diagnostic reference levels for multi detector computed tomography*, Australas Phys Eng Sci Med 36:19-26. doi: 10.1007/s13246-013-0180-6
7. Australian Radiation Protection and Nuclear Safety Agency (ARPANSA), 2005. *Code of practice – Exposure of humans to ionising radiation for research purposes*, Radiation Protection Publication Series No. 8, ARPANSA, Yallambie.
8. International Electrotechnical Commission (IEC), 2005. *Medical Diagnostic X-ray Equipment – Radiation Conditions for Use in the Determination of Characteristics*, IEC 61267, IEC, Geneva
9. International Atomic Energy Agency, 2007. *Dosimetry in Diagnostic Radiology: An International Code of Practice*, IAEA Technical Report Series 457, Vienna
10. Hourdakis CJ, Csete I, Dures J et al, 2015. *Comparison of air kerma area product and air kerma meter calibrations for X-ray radiation qualities used in diagnostic radiology*, Metrologica 52 Tech Suppl, 06024:1-98
11. Csete I, Büermann L, Alikhani B, Gomola I, 2015. *Comparison of air kerma-length product measurements between the PTB and the IAEA for X-radiation qualities used in computed tomography*, Metrologica 52 Tech Suppl, 06014:1-13
12. Csete I, Büermann L, Gomola I, Girzikowsky R, 2013. *Comparison of air kerma measurements between the PTB and the IAEA for X-radiation qualities used in general diagnostic radiology and mammography*, Metrologica 50 Tech Suppl, 06008:1-16
13. Kessler C, Burns D, Czap L, Csete I, Gomola I, 2013. *Comparison of air kerma standards of the IAEA and BIPM in mammography X-rays*, Metrologica 50 Tech Suppl, 06005:1-9
14. Meghzifenea A, Danceb DR, McLeana D, Kramer H M, 2010. *Dosimetry in Diagnostic Radiology*, European Journal of Radiology, 76:11-14
15. Deutsches Institut Fur Normung E.V., 1988. *German Standard DIN6809-4 Clinical dosimetry; applications of X-rays with peak voltages between 10 and 100 kV in radiotherapy and soft tissue diagnostics*, German National Standard
16. International Organization for Standardization, 1996. *X and gamma reference radiation for calibrating dosimeters and doserate meters and for determining their response as a function of photon energy – Part 1: Radiation characteristics and production methods*, ISO 4037-1
17. International Organization for Standardization, 1997. *X and gamma reference radiation for calibrating dosimeters and doserate meters and for determining their response as a function of photon energy –*

Part 2: Dosimetry for radiation protection over the energy ranges from 8 keV to 1.3 MeV and 4 MeV to 9 MeV, ISO 4037-2

18. International Organization for Standardization, 1999. *X and gamma reference radiation for calibrating dosimeters and doserate meters and for determining their response as a function of photon energy – Part 3: Calibration of area and personal dosimeters and the measurement of their response as a function of energy and angle of incidence*, ISO 4037-3
19. Lee KL, Butler D, Bailey T, 2017. *Establishing IAEA TRS-457 Diagnostic X-ray Beam Qualities at the Australian Primary Standard Dosimetry Laboratory*, APESM 40(4):881-893, <https://doi.org/10.1007/s13246-017-0604-9>
20. PTW, 2014, *SFD chambers Type 34060 and Type 34069 user manual*, PTW-Freiburg, Germany.
21. Lye JE, Butler DJ, Webb DV, 2010, *Monte Carlo correction factors for the ARPANSA kilovoltage free-air chambers and the effect of moving the limiting aperture*. *Metrologica*, 47:11-20, doi:10.1088/0026-1394/47/1/002
22. Burns DT, Büermann L 2009, *Free-air ionization chambers*. *Metrologica*, 46:S9-S23, doi:10.1088/0026-1394/46/2/S02.
23. PTW, 2014. *Nomex user manual*, PTW-Freiburg, Germany.
24. Burns DT, Lye JE, Roger P, Butler DJ, 2012. *Key comparison BIPM.RI(I)-K3 of the air-kerma standards of the ARPANSA, Australia and the BIPM in medium-energy X-rays*, *Metrologica* 49 Tech Suppl, 06007:1-15.
25. ICRU, 2014. *ICRU Report 90 Key Data for Ionizing-Radiation Dosimetry: Measurement Standards and Applications*, *Journal of the ICRU* 14(1), Oxford University Press
26. Joint Committee for Guides in Metrology 2010. *Evaluation of Measurement Data – Guide to the Expression of Uncertainty in Measurement*, JCGM 100:2008.
27. Punnoose J, Xu J, Sisniegav A, Zbijewski W, and Siewerdsen JH, 2016. *Technical Note: spektr 3.0—A computational tool for x-ray spectrum modeling and analysis*, *Medical Physics* 43(8), 4711 – 4717, doi: 10.1118/1.4955438.
28. Hopewell Designs Inc, 2015. *System Manual for the X80-320-A X-ray Irradiator System*, Hopewell Designs Inc, Alpharetta.
29. PTW 2006. *Unidos webline Type 10021, Type 10022 and Type 10023, firmware 2.06 or higher user manual*, PTW-Freiburg, Germany.